JCI The Journal of Clinical Investigation

Prostaglandin E_2 reduces radiation-induced epithelial apoptosis through a mechanism involving AKT activation and bax translocation

Teresa G. Tessner, … , Shrikant Anant, William F. Stenson

J Clin Invest. 2004;114(11):1676-1685. https://doi.org/10.1172/JCI22218.

Article

Prostaglandin E_2 (PGE_2) synthesis modulates the response to radiation injury in the mouse intestinal epithelium through effects on crypt survival and apoptosis; however, the downstream signaling events have not been elucidated. WT mice receiving 16,16-dimethyl PGE_2 ($dmPGE_2$) had fewer apoptotic cells per crypt than untreated mice. Apoptosis in $Bax^{-/-}$ mice receiving 12 Gy was approximately 50% less than in WT mice, and the ability of $dmPGE_2$ to attenuate apoptosis was lost in $Bax^{-/-}$ mice. Positional analysis revealed that apoptosis in the $Bax^{-/-}$ mice was diminished only in the bax-expressing cells of the lower crypts and that in WT mice, $dmPGE_2$ decreased apoptosis only in the bax-expressing cells. The HCT-116 intestinal cell line and $Bax^{-/-}$ HCT-116 recapitulated the apoptotic response of the mouse small intestine with regard to irradiation and $dmPGE_2$. Irradiation of HCT-116 cells resulted in phosphorylation of AKT that was enhanced by $dmPGE_2$ through transactivation of the EGFR. Inhibition of AKT phosphorylation prevented the reduction of apoptosis by $dmPGE_2$ following radiation. Transfection of HCT-116 cells with a constitutively active AKT reduced apoptosis in irradiated cells to the same extent as in nontransfected cells treated with $dmPGE_2$. Treatment with $dmPGE_2$ did not alter bax or bcl-x expression but suppressed bax translocation to the mitochondrial membrane. Our in vivo studies indicate that there are bax-dependent and bax-independent radiation-induced apoptosis in the […]

Prostaglandin E_2 reduces radiation-induced epithelial apoptosis through a mechanism involving AKT activation and bax translocation

Teresa G. Tessner, Filipe Muhale, Terrence E. Riehl, Shrikant Anant, and William F. Stenson

Division of Gastroenterology, Department of Internal Medicine, Washington University School of Medicine, St. Louis, Missouri, USA.

Prostaglandin E_2 (PGE_2) synthesis modulates the response to radiation injury in the mouse intestinal epithelium through effects on crypt survival and apoptosis; however, the downstream signaling events have not been elucidated. WT mice receiving 16,16-dimethyl PGE_2 ($dmPGE_2$) had fewer apoptotic cells per crypt than untreated mice. Apoptosis in *Bax*$^{-/-}$ mice receiving 12 Gy was approximately 50% less than in WT mice, and the ability of $dmPGE_2$ to attenuate apoptosis was lost in *Bax*$^{-/-}$ mice. Positional analysis revealed that apoptosis in the *Bax*$^{-/-}$ mice was diminished only in the bax-expressing cells of the lower crypts and that in WT mice, $dmPGE_2$ decreased apoptosis only in the bax-expressing cells. The HCT-116 intestinal cell line and *Bax*$^{-/-}$ HCT-116 recapitulated the apoptotic response of the mouse small intestine with regard to irradiation and $dmPGE_2$. Irradiation of HCT-116 cells resulted in phosphorylation of AKT that was enhanced by $dmPGE_2$ through transactivation of the EGFR. Inhibition of AKT phosphorylation prevented the reduction of apoptosis by $dmPGE_2$ following radiation. Transfection of HCT-116 cells with a constitutively active AKT reduced apoptosis in irradiated cells to the same extent as in nontransfected cells treated with $dmPGE_2$. Treatment with $dmPGE_2$ did not alter bax or bcl-x expression but suppressed bax translocation to the mitochondrial membrane. Our in vivo studies indicate that there are bax-dependent and bax-independent radiation-induced apoptosis in the intestine but that only the bax-dependent apoptosis is reduced by $dmPGE_2$. The in vitro studies indicate that $dmPGE_2$, most likely by signaling through the E prostaglandin receptor EP_2, reduces radiation-induced apoptosis through transactivation of the EGFR and enhanced activation of AKT and that this results in reduced bax translocation to the mitochondria.

Introduction

The small-intestinal epithelium is continuously replaced by the replication of transit cells in the crypt and the subsequent migration of their progeny to the villous epithelium (reviewed in ref. 1). Radiation injury kills the replicating transit cells, but some stem cells in the base of the crypt survive. These surviving stem cells play a central role in the regeneration of the crypts and eventually the entire mucosa after radiation injury (reviewed in ref. 2). Higher doses of radiation kill more stem cells and reduce the number of regenerative crypts.

Cells respond to radiation-induced DNA damage with cell cycle arrest, DNA repair, and apoptosis (reviewed in refs. 3–5). Exogenous agents can modulate the pattern of cellular response to radiation. Prostaglandin E_2 (PGE_2) is radioprotective for intestinal epithelium; that is, administration of 16,16-dimethyl PGE_2 ($dmPGE_2$), a stable analog of PGE_2, prior to radiation increases the number of surviving crypts after radiation (6, 7). The increased crypt survival seen with PGE_2 signaling correlates with diminished radiation-induced apoptosis (8, 9). The radioprotective effects of PGE_2 have practical consequences for radiation therapy (reviewed in refs. 10, 11). COX, the central enzyme in PG synthesis, has 2 isoforms, COX-1 and COX-2. Many colon cancers express COX-2, resulting in increased PGE_2 production and decreased sensitivity to radiation therapy (11). Administration of selective COX-2 inhibitors prior to radiation increases the sensitivity of COX-2–expressing tumors to radiation therapy (12–16). The mechanisms by which COX-2 expression and PGE_2 production affect the response to radiation therapy are not known.

We found that PGE_2 synthesis plays a critical role in the response to radiation injury by the normal mouse intestinal epithelium. Administration of indomethacin, which inhibits both COX-1 and COX-2, in the period 24–48 hours after radiation significantly decreased the number of surviving small-intestinal crypts (17). Irradiated COX-1 knockout mice have decreased intestinal crypt survival and increased apoptosis compared with their WT littermates, demonstrating an important role for PGs produced through COX-1 in regulating radiation-induced apoptosis (8). Studies with E prostaglandin (EP) receptor knockout mice demonstrate that the effects of PGE_2 on radiation-induced apoptosis and crypt survival are mediated through the EP_2 receptor (9); however, the downstream signaling events initiated by PG signaling have not been elucidated.

PGE_2 elicits cellular responses via G-coupled 7–transmembrane domain receptors of 4 subtypes: EP_1, EP_2, EP_3, and EP_4 (reviewed in ref. 18). EP_2 and EP_4 were originally distinguished by their ability to increase cAMP levels (reviewed in ref. 19). EP_2 mediates the reduction of apoptosis and the enhancement of crypt survival observed in the intestine of $dmPGE_2$-treated irradiated mice (9). One possible signaling pathway for the effects of PGE_2 on apoptosis is the phosphorylation of AKT, a ubiquitously expressed serine/threonine kinase that is downstream of PI3K (reviewed in ref. 20). Signaling through EP_2 or EP_4 is coupled to activation of

Nonstandard abbreviations used: $dmPGE_2$, 16,16-dimethyl PGE_2; EP, E prostaglandin; MEK, mitogen-activated/extracellular-regulated kinase; myrAKT, myristoyl-AKT; PGE_2, prostaglandin E_2; siRNA, small interfering RNA.

Conflict of interest: The authors have declared that no conflict of interest exists.

Citation for this article: *J. Clin. Invest.* **114**:1676–1685 (2004). doi:10.1172/JCI200422218.

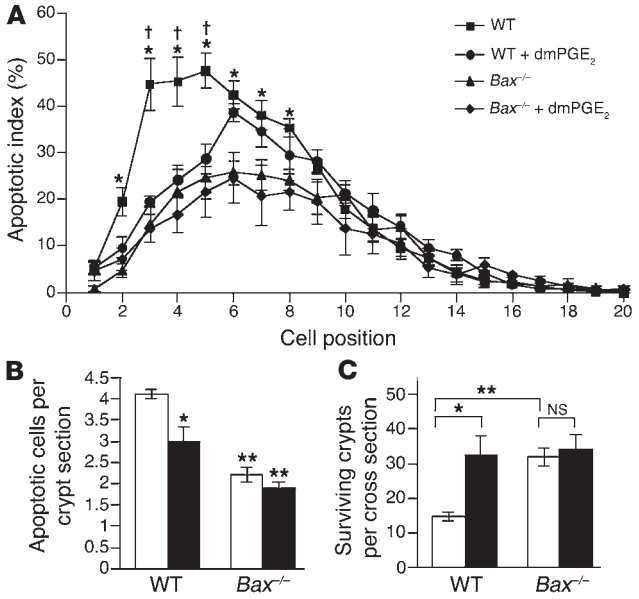

Figure 1
Apoptosis and crypt survival in $dmPGE_2$-treated irradiated WT and *Bax*$^{-/-}$ mice. (**A**) Apoptotic index. WT or *Bax*$^{-/-}$ mice received vehicle or $dmPGE_2$ (0.5 mg/kg) 1 hour prior to irradiation (12 Gy). Mice were killed 6 hours after radiation, and the cell-positional distribution of apoptosis in the crypts was scored. Data are the mean ± SEM. *$P < 0.05$, WT compared with *Bax*$^{-/-}$ or with *Bax*$^{-/-}$ plus $dmPGE_2$; †$P < 0.05$, WT compared with WT plus $dmPGE_2$, *Bax*$^{-/-}$, or *Bax*$^{-/-}$ plus $dmPGE_2$. WT, $n = 8$; WT plus $dmPGE_2$, $n = 4$; *Bax*$^{-/-}$, $n = 6$; *Bax*$^{-/-}$ plus $dmPGE_2$, $n = 4$. (**B**) Apoptotic cells in small-intestinal crypts 6 hours after radiation. WT or *Bax*$^{-/-}$ mice received vehicle (white bars) or $dmPGE_2$ (black bars) 1 hour prior to irradiation. Mice were killed 6 hours after radiation, and the number of apoptotic cells per crypt was scored. Data are the mean ± SEM. *$P < 0.05$; **$P < 0.0001$ compared with WT plus vehicle. WT plus vehicle, $n = 16$; WT plus $dmPGE_2$, $n = 4$; *Bax*$^{-/-}$ plus vehicle, $n = 7$; *Bax*$^{-/-}$ plus $dmPGE_2$, $n = 4$. (**C**) Crypt survival. WT or *Bax*$^{-/-}$ mice received vehicle (white bars) or $dmPGE_2$ (black bars) 1 hour prior to irradiation. Mice were killed 84 hours after radiation, and the number of surviving crypts per cross section was scored. Data are the mean ± SEM. *$P < 0.05$; **$P < 0.0001$. WT plus vehicle, $n = 7$; WT plus $dmPGE_2$, $n = 4$; *Bax*$^{-/-}$ plus vehicle, $n = 12$; *Bax*$^{-/-}$ plus $dmPGE_2$, $n = 8$.

AKT (21). AKT phosphorylation mediates antiapoptotic and prosurvival events (reviewed in refs. 20, 22, 23). Phosphorylated AKT inactivates proapoptotic proteins including bad, caspase-9, and forkhead and activates antiapoptotic proteins including NF-κB and cAMP response element–binding protein (20). The possible inactivation of the proapoptotic protein bax by phosphorylated AKT is of particular interest, because bax mediates radiation-induced apoptosis in the CNS (24) and ovarian and pancreatic cancer cell lines (25, 26). Bax is expressed in the cells at the base of the intestinal epithelial crypt (27–29). Under resting conditions, bax is localized in the cytoplasm. In response to proapoptotic signals, including radiation, bax translocates to the mitochondria, where it permeabilizes the mitochondrial membrane, resulting in the release of cytochrome *c* and apoptosis (reviewed in refs. 30–32). Recent studies indicate that AKT signaling prevents bax translocation to the mitochondria (33, 34) via direct phosphorylation of Ser 184 (35). Bax mediates apoptosis induced by chemotherapeutic agents in the intestinal cell line HCT-116 (36), and bax translocation is associated with radiation-induced apoptosis in mouse thymocytes (37). However, the 1 study that addressed the role of bax in mediating radiation-induced apoptosis in the intestine suggested that it was not involved (38).

In this study we attempted to define the downstream signaling events that mediate the antiapoptotic effects of PGE_2 in the intestinal epithelium. We focused on AKT phosphorylation and the inhibition of bax translocation as possible mediators of the effects of PGE_2 on apoptosis, because AKT and bax are known to play key roles in radiation-induced apoptosis (5, 20, 30). Using *Bax*$^{-/-}$ mice, we found that there was both bax-dependent and bax-independent radiation-induced apoptosis in the intestine and that only the bax-dependent apoptosis was blocked by $dmPGE_2$; moreover, positional analysis of apoptosis demonstrated that PGE_2 only affected apoptosis in the bax-expressing cells at the base of the crypt. HCT-116 cells were used to define the intermediate steps in the inhibition of apoptosis in cells treated with $dmPGE_2$ prior to irradiation. We found that in HCT-116 cells administration of $dmPGE_2$ activates AKT phosphorylation, which, in turn, blocks the translocation of bax from the cytoplasm to the mitochondria.

Results

We had previously demonstrated that $dmPGE_2$ decreases radiation-induced apoptosis in the small intestine. To determine whether bax mediates the effects of $dmPGE_2$ on radiation-induced apoptosis, we administered $dmPGE_2$ to WT and *Bax*$^{-/-}$ mice prior to irradiation and performed positional analysis of apoptosis. The apoptotic index in WT C57BL/6 mice was markedly increased 6 hours following 12 Gy irradiation (Figure 1A). The apoptotic index was highest for cell positions 3–5 (corresponding to the putative position of the crypt stem cell) and gradually decreased at positions higher in the crypt. One-way ANOVA indicated statistically significant differences for cell positions 2–8 (Table 1). Treatment of WT mice with $dmPGE_2$ prior to irradiation resulted in a reduced apoptotic index for cell positions 3–5 (Figure 1A). However, the apoptotic index for cell positions higher in the crypt was unaffected. Irradiated *Bax*$^{-/-}$ mice exhibited a reduction in apoptotic index for cell positions 2–8 compared with WT mice. Treatment of *Bax*$^{-/-}$ mice with $dmPGE_2$ did not result in any further change in apoptotic index. The total number of apoptotic cells per crypt after irradiation was also reduced in $dmPGE_2$-treated WT mice compared with untreated mice (Figure 1B), but the reduction was less striking than that seen in the positional analysis. Similarly, the number of apoptotic cells per crypt was reduced

Table 1
Statistical significance of treatment-group differences in cell-positional apoptotic index

CP	WT + $dmPGE_2$	*Bax*$^{-/-}$	*Bax*$^{-/-}$ + $dmPGE_2$
2	0.084	0.002	0.023
3	0.010	0.001	0.002
4	0.043	0.009	0.005
5	0.034	0.003	0.003
6	0.867	0.005	0.008
7	0.910	0.031	0.023
8	0.545	0.040	0.025

Data are *P* values versus WT by 1-way ANOVA analysis. CP, cell position.

Table 2
Percent apoptosis in HCT-116 and *Bax*$^{-/-}$ HCT-116 cells

Treatment	HCT-116	HCT-116 + LY294002	*Bax*$^{-/-}$	*Bax*$^{-/-}$ + LY294002
Vehicle	7.6 ± 0.3	11.3 ± 0.6	5.9 ± 0.3[D]	10.1 ± 1.0
$dmPGE_2$	5.6 ± 0.3[A]	10.8 ± 0.5	6.4 ± 0.3	9.8 ± 0.3
6 Gy	20.0 ± 1.0[A]	23.4 ± 1.2	13.8 ± 0.5[E]	18.9 ± 0.3[F]
6 Gy + $dmPGE_2$	9.3 ± 0.4[A,B]	23.6 ± 0.4[C]	10.8 ± 1.3	20.3 ± 0.2

Apoptosis was determined 24 hours after treatment by flow cytometry using annexin V–FITC and propidium iodide staining. Where indicated, cells received 10 μM $dmPGE_2$ and/or 10 μM LY294002 prior to irradiation. Data are average percent apoptosis ± SEM (n = 4–15) determined in at least 2 separate experiments. [A]$P < 0.005$ compared with HCT-116 plus vehicle. [B]$P < 0.0001$ compared with 6 Gy. [C]$P < 0.0001$ compared with irradiated HCT-116 plus $dmPGE_2$. [D]$P < 0.005$ compared with HCT-116 plus vehicle. [E]$P < 0.0002$ compared with HCT-116 plus 6 Gy. [F]$P < 0.0005$ compared with irradiated *Bax*$^{-/-}$.

in *Bax*$^{-/-}$ mice with no further effect of $dmPGE_2$. The reduction in total number of apoptotic cells per crypt in *Bax*$^{-/-}$ mice compared with WT (approximately 50%) was larger than that induced by $dmPGE_2$ treatment of WT mice and probably reflects the additional reduction in apoptosis at cell positions 6–8 that was observed in *Bax*$^{-/-}$ mice. For both $dmPGE_2$-treated WT and *Bax*$^{-/-}$ mice, the reduction in apoptosis correlated with a comparable increase in crypt survival (Figure 1C).

The suitability of HCT-116 cells, a transformed human colon cancer cell line, as a model of mouse intestinal epithelial apoptosis was tested by determination of the apoptotic response of these cells and *Bax*$^{-/-}$ HCT-116 cells to irradiation in the presence and absence of $dmPGE_2$ (Table 2). Irradiation (6 Gy) increased the percentage of apoptotic HCT-116 cells from approximately 8% to approximately 20%, and this apoptosis was reduced by $dmPGE_2$ treatment (6 Gy, 20.0%; 6 Gy plus $dmPGE_2$, 9.3%). The apoptotic response of HCT-116 p21 parental cells and HCT-116 *Bax*$^{+/-}$ cells that were unirradiated, irradiated, or irradiated in the presence of $dmPGE_2$ was the same as that of similarly treated HCT-116 cells (data not shown). Additionally, *Bax*$^{-/-}$ HCT-116 cells exhibited less apoptosis (13.8%) following radiation compared with HCT-116 cells (20.0%). Treatment with $dmPGE_2$ did not further reduce apoptosis in the *Bax*$^{-/-}$ cells (Table 2). Radiation-induced apoptosis was reduced but not eliminated in the *Bax*$^{-/-}$ HCT-116 cells. This suggests that in HCT-116 cells, as in the mouse intestine, there is bax-dependent and bax-independent radiation-induced apoptosis. HCT-116 and *Bax*$^{-/-}$ HCT-116 cells also recapitulated the effect of $dmPGE_2$ on radiation-induced apoptosis in the mouse small intestine (compare Table 2 and Figure 1).

We then used HCT-116 cells as a model to define the intracellular signaling events that mediate the effects of $dmPGE_2$ on radiation-induced apoptosis. The first signaling pathway we investigated was the PI3K/AKT pathway, which modulates several points in the apoptotic cascade, including the function of anti- and proapoptotic bcl-2 family members. We assessed the activation of AKT in the intestinal cell line HCT-116 following irradiation at 6 Gy in the presence or absence of $dmPGE_2$ using a phosphospecific AKT antibody and correcting for total AKT expression. In unirradiated cells, $dmPGE_2$ enhanced AKT phosphorylation to a level comparable to that observed in HCT-116 cells receiving only 6 Gy (data not shown). Treatment of HCT-116 cells with $dmPGE_2$ just prior to irradiation resulted in AKT Ser 473 phosphorylation, which increased approximately threefold at 12 hours compared with that in irradiated HCT-116 cells not receiving $dmPGE_2$ (Figure 2). Western analysis of HCT-116 indicated that these cells express all 4 EP receptor subtypes (data not shown); therefore we used receptor-specific agonists to determine which EP receptor was responsible for the increased AKT phosphorylation observed with $dmPGE_2$ treatment. The receptor-specific agonists tested were butaprost (for EP_2), PGE_1 alcohol (for EP_4), and 17-phenyltrinor-PGE_2 (for EP_1 and EP_3). Each agonist was used at a concentration above its K_I (18) and at a concentration previously shown to activate its target receptor in gastrointestinal cell lines (39–41). Tenfold higher concentrations of the agonists shown in Figure 2 either were toxic or had no effect on AKT phosphorylation (data not shown). Only the EP_2-selective agonist, butaprost, resulted in AKT phosphorylation comparable to that observed in $dmPGE_2$-treated HCT-116 cells (Figure 2).

EP_2 activation and EP_4 activation have been linked to increased phosphorylation of AKT (19, 21); however, the transduction events mediating this event remain unclear. Transactivation of the EGFR in response to PGE_2 signaling occurs in several gastrointestinal cell lines (42, 43) and results in AKT phosphorylation in LS174T cells via an src-dependent pathway (43). Therefore we determined

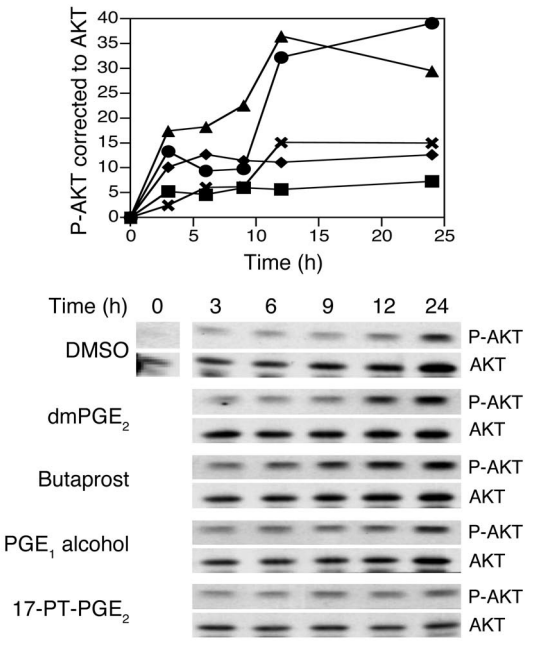

Figure 2
Effect of radiation and PGE_2 analogs on AKT phosphorylation. HCT-116 cells were treated with DMSO, 10 μM $dmPGE_2$, or one of the EP receptor agonists, butaprost (10 μM), PGE_1 alcohol (1 μM), or 17-phenyltrinor-PGE_2 (17-PT-PGE_2; 10 μM), irradiated at 6 Gy, and lysed at the indicated times. Duplicate lysates were combined, proteins were separated by SDS-PAGE, and phosphorylated AKT (P-AKT) was detected using a phosphospecific antibody. Blots were stripped and reprobed for AKT. Upper panel: Densitometry of Western blot, showing phospho-AKT (P-AKT) corrected to total AKT. Squares, DMSO; circles, $dmPGE_2$; triangles, butaprost; diamonds, PGE_1 alcohol; X's, 17-phenyltrinor-PGE_2. Lower panel: Representative Western blot. Data are representative of at least 3 separate experiments.

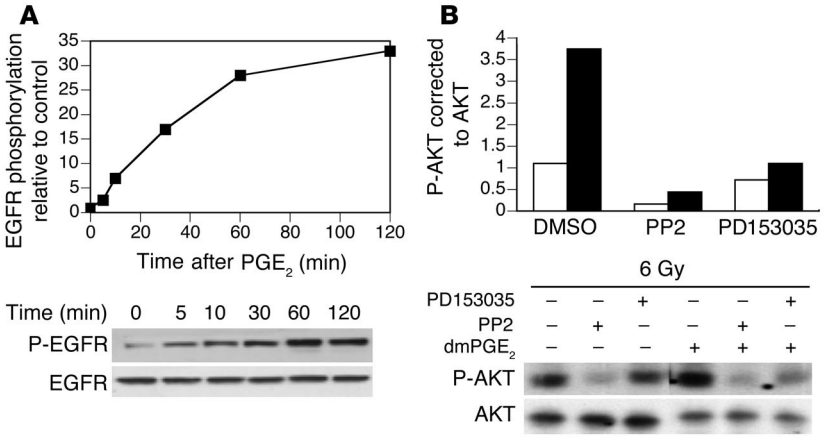

Figure 3
Stimulation of AKT phosphorylation by $dmPGE_2$ is dependent on src activity and transactivation of the EGFR. (**A**) Treatment of HCT-116 cells with $dmPGE_2$ results in phosphorylation of the EGFR at Tyr 1068. EGFR expression and phospho-EGFR (P-EGFR; Tyr 1068) expression in cell lysates treated for the indicated times with 1 μM $dmPGE_2$ were determined by Western analysis using specific antibodies. Upper panel: Phospho-EGFR expression corrected to total EGFR expression. Lower panel: Representative Western blot. Data are representative of 3 separate experiments. (**B**) Inhibition of src or EGFR kinase activity inhibits phosphorylation of AKT in response to $dmPGE_2$. HCT-116 cells were pretreated 1 hour with either 10 μM PP2 (src inhibitor) or 1 μM PD153035 (EGFR kinase inhibitor) and then irradiated at 6 Gy in the presence (black bars) or absence (white bars) of 10 μM $dmPGE_2$. Duplicate cell lysates were combined, and Western blot analysis was used to determine the amounts of phospho-AKT and AKT. Upper panel: Densitometry of phospho-AKT corrected for total AKT expression. Lower panel: Representative Western blot.

whether this mechanism wvas responsible for the enhanced phosphorylation of AKT in $dmPGE_2$-treated HCT-116 cells. As shown in Figure 3A, $dmPGE_2$ treatment of HCT-116 cells enhanced EGFR phosphorylation. Both the src inhibitor PP2 and the EGFR kinase inhibitor PD153035 dramatically attenuated $dmPGE_2$-stimulated AKT phosphorylation in irradiated HCT-116 cells (Figure 3B). The ability of $dmPGE_2$ to enhance the phosphorylation of AKT in irradiated HCT-116 cells (Figure 2) suggested that the PI3K/AKT signaling cascade is responsible for the decrease in (bax-dependent) apoptosis observed in $dmPGE_2$-treated mice. Consistent with the central role of PI3K/AKT in cell survival, the PI3K inhibitor LY294002 increased baseline apoptosis in both HCT-116 and *Bax*$^{-/-}$ HCT-116 cells (Table 2). However, LY294002 treatment did not further increase apoptosis in irradiated HCT-116 cells. LY294002 treatment of irradiated *Bax*$^{-/-}$ HCT-116 cells increased the level of apoptosis to nearly that of irradiated HCT-116 cells consistent with the ability of PI3K/AKT to also modulate apoptosis through targets other than bax. LY294002 abrogated the ability of $dmPGE_2$ to reduce radiation-induced apoptosis in HCT-116 cells (Table 2). $dmPGE_2$ was unable to reduce apoptosis in irradiated *Bax*$^{-/-}$ HCT-116 cells treated with LY294002 (Table 2). Taken together, these data suggest that the ability of $dmPGE_2$ to reduce apoptosis after radiation injury requires AKT activation and subsequent modulation of bax function.

To confirm the suggested link between $dmPGE_2$-induced phosphorylation of AKT and a reduction in radiation-induced apoptosis, we used a genetic approach to modulate AKT specifically. HCT-116 cells transfected with an empty vector plasmid displayed baseline and radiation-induced apoptosis comparable to that of nontransfected cells (compare Tables 2 and 3). HCT-116 cells transfected with an expression vector of AKT containing a myristoylation sequence so that AKT is constitutively active showed an approximately 50% reduction in apoptosis in response to 6 Gy compared with HCT-116 cells transfected with control plasmid (Table 3). This reduction in apoptosis was comparable to that observed for nontransfected HCT-116 cells receiving $dmPGE_2$ prior to radiation (compare Tables 2 and 3). We next used small interfering RNA (siRNA) technology to specifically knock down AKT expression. Transfection of HCT-116 cells with a scrambled control siRNA had no effect on baseline apoptosis, and these cells underwent apoptosis in response to radiation in the presence and absence of $dmPGE_2$ to an extent similar to that in nontransfected HCT-116 cells (compare Tables 2 and 3). Transfection of HCT-116 cells with an AKT siRNA for 48 hours reduced AKT protein levels approximately 80% (data not shown). While baseline apoptosis was unaffected by AKT siRNA transfection, apoptosis following 6 Gy was double that observed in nontransfected irradiated cells (compare Tables 2 and 3). The enhanced apoptotic response of irradiated cells in which AKT has been knocked down compared with irradiated cells in which PI3K is inhibited with LY294002 is consistent with a role for PI3K-indepedent AKT activation in response to stress. Like LY294002-treated nontransfected cells, $dmPGE_2$ did not reduce the apoptotic response to irradiation in AKT siRNA–transfected cells. In contrast to LY294002 treatment, AKT siRNA treatment did not alter baseline apoptosis. These findings are consistent with the ability of PI3K to activate signaling pathways important in growth and proliferation, other than AKT, such as ras, rac, and MAPK (reviewed in refs. 44, 45).

The experiments assessing the effects of LY294002 on radiation-induced apoptosis in HCT-116 and *Bax*$^{-/-}$ HCT-116 cells suggest that the effects of AKT phosphorylation on apoptosis may be mediated through effects on bax. The apoptotic effects of bax are mediated by its migration from the cytoplasm to the mitochondria. Therefore we determined bax localization following irradiation in the presence and absence of $dmPGE_2$, and the effect of altered AKT activity on this localization. Mitochondrial and cytosolic fractions were obtained, and bax protein in the cytosol was routinely tracked, since markers to assess the purity of the mitochondrial fraction are problematic. In the absence of irradiation, bax was localized to the cytoplasm (Figure 4). The amount of bax in the cytosol was reduced by more than 90% 24 hours after 6 Gy radiation. However, in HCT-116 cells receiving $dmPGE_2$ prior to irradiation, the amount of bax in the cytosol remained unchanged (Figure 4A). Bax remained in the cytosol after irradiation of HCT-116 cells transfected with a constitutively active AKT construct, myristoyl-AKT (myrAKT) (Figure 4A). $dmPGE_2$ treatment did not further enhance the localization of bax to the cytosol in myrAKT-transfected cells; this indicates a primary role of AKT in mediating the PGE_2-induced retention of bax in the cytosol. Conversely, there was no detectable cytosolic bax when irradiated cells were treated with LY294002. Consistent with PI3K/AKT signaling as a downstream effector for $dmPGE_2$, bax translocation from the

Table 3
Percent apoptosis in HCT-116 cells with altered AKT expression

Treatment	pcDNA	myr-AKT	Scrambled siRNA	AKT siRNA
Vehicle	8.0 ± 0.6	7.3 ± 0.6	8.5 ± 0.9	7.1 ± 0.9
$dmPGE_2$			6.6 ± 0.2	6.8 ± 0.8
6 Gy	27.2 ± 1.3	12.0 ± 0.8[A]	20.2 ± 0.4	43.6 ± 2.9[B]
6 Gy + $dmPGE_2$			9.8 ± 1.0	44.2 ± 2.9[B]

Percent apoptosis was determined as in Table 2. Cells were incubated for 24 hours in the presence of siRNA followed by a further 24 hours in the presence of fresh medium. The cells were then used for radiation-induced apoptosis experiments as described in Methods. Data are the average ± SEM (n = 5–12) determined from at least 2 separate experiments. [A]$P < 0.0001$ compared with irradiated pcDNA-transfected. [B]$P \leq 0.001$ compared with comparable treatment in HCT-116 cells transfected with scrambled siRNA.

cytosol in irradiated LY294002-treated cells was not prevented by $dmPGE_2$. Analysis of bax expression in both the cytosolic and the mitochondrial fractions demonstrated that the loss of cytosolic bax in irradiated cells was accompanied by an increase in the amount of bax associated with the mitochondrial fraction (Figure 4B). Furthermore, the relative distribution of cytosolic and mitochondrial bax in HCT-116 cells irradiated in the presence of $dmPGE_2$ was similar to that in unirradiated cells (Figure 4B). As PI3K/AKT signaling also regulates the expression of pro- and antiapoptotic proteins, we determined the expression of bax (Figure 4C) and bcl-x (Figure 4D) in HCT-116 cells irradiated in the presence and absence of $dmPGE_2$. There was a gradual increase in both bax and bcl-x protein levels in the 24 hours following radiation; however, $dmPGE_2$ did not alter the expression of these 2 proteins (Figure 4, C and D). Thus, it is most likely that the predominant means by which $dmPGE_2$ reduces apoptosis in irradiated intestinal cells is modulation of bax translocation to the mitochondria.

Ionizing radiation variably activates different MAPK signaling modules depending upon the cell type. Likewise, these pathways may differentially contribute to enhancing or attenuating apoptosis. Western blotting analysis revealed that 6 Gy radiation induced phosphorylation of ERK within 2 hours. Maximal phosphorylation occurred 6 hours following radiation (Figure 5). The mitogen-activated/extracellular-regulated kinase (MEK) 1/2 inhibitor UO126 completely prevented radiation-induced ERK phosphorylation (Figure 5). Total ERK protein levels did not change over the observation period (Figure 5). Likewise, p38 and JNK protein levels did not change (Figure 5). We were unable to detect phosphorylation of either p38 or JNK using 2 different phosphospecific antibodies. We used small-molecule inhibitors of p38 MAPK (SB203580), MEK 1/2 (UO126; ERK pathway), and JNK (SP600125) to assess the ability of these pathways to modulate $dmPGE_2$ attenuation of radiation-induced apoptosis in HCT-116 cells. Treatment of HCT-116 cells with these inhibitors resulted in little if any increase or decrease in

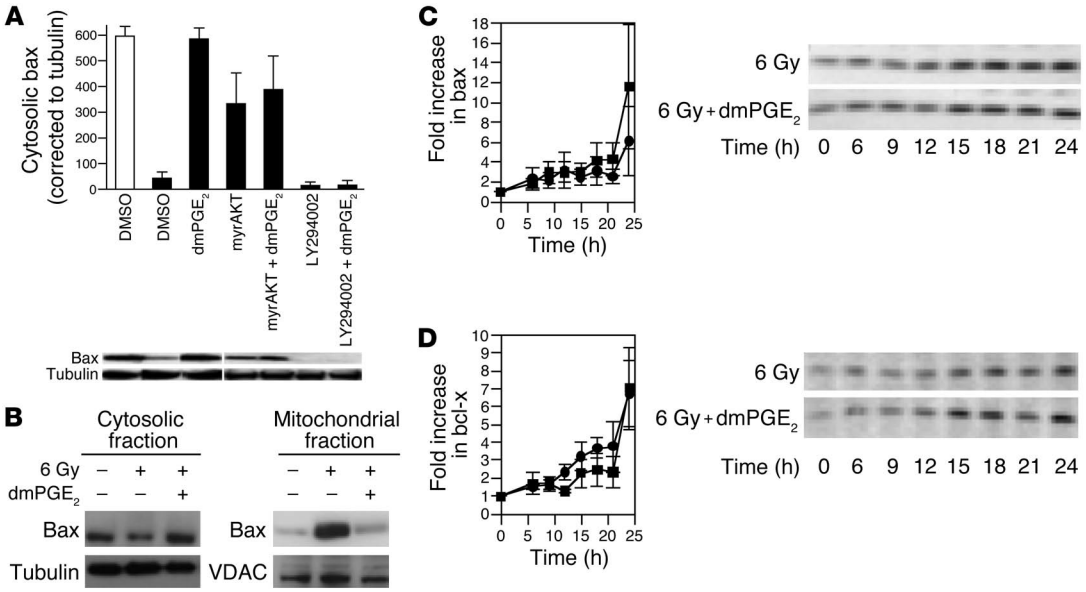

Figure 4
Bax translocation but not bax or bcl-x expression is modulated in irradiated HCT-116 cells by $dmPGE_2$.(**A**) Bax translocation in HCT-116 cells. HCT-116 cells or HCT-116 cells transfected with a constitutively active AKT construct (myrAKT) received DMSO or $dmPGE_2$ (10 μM) 1 hour prior to 6 Gy irradiation (black bars, 6 Gy; white bar, unirradiated). Where indicated, HCT-116 cells received 10 μM LY294002 1 hour prior to $dmPGE_2$ treatment and subsequent irradiation. Twenty-four hours after irradiation, cells were isolated and fractionated into cytosolic and mitochondrial fractions, and the cytosolic fraction was analyzed for bax by Western blotting analysis. Upper panel: Average (± range) densitometry from 2 separate blots. Lower panel: Representative Western blot. (**B**) Translocation of bax from the cytosol to mitochondria in irradiated HCT-116 cells. Cytosolic and mitochondrial fractions were prepared from unirradiated HCT-116 cells and cells irradiated in the presence or absence of 10 μM $dmPGE_2$. Proteins were separated by SDS-PAGE, and Western blots were probed for bax, tubulin, and voltage-dependent anion-selective channel protein (VDAC) as indicated. Data are representative of 2 separate experiments. (**C** and **D**) Bax (**C**) and bcl-x (**D**) expression in HCT-116 cells. HCT-116 cells were treated with DMSO or $dmPGE_2$ (10 μM), irradiated at 6 Gy, and lysed at the indicated times. Duplicate lysates were combined, proteins were separated by SDS-PAGE, and bax or bcl-x expression levels were detected by Western blotting. Left panels: Densitometric analysis of several blots. Squares, vehicle; circles, $dmPGE_2$. Data are the average ± SEM for 3–4 separate blots. Right panels: Representative Western blot.

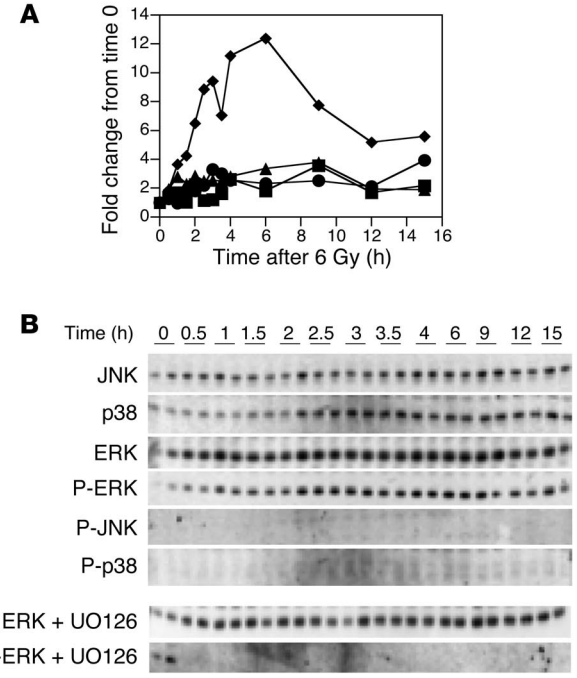

Figure 5
Effect of radiation on MAPK expression and phosphorylation. HCT-116 cells were irradiated at 6 Gy and lysed at the indicated times. Duplicate lysates were separated by SDS-PAGE, and nonphosphorylated and phosphorylated JNK, p38 MAPK, and ERK were detected using antibodies against the nonphosphorylated and phosphorylated (P-) forms of the kinases. (**A**) Densitometry of Western blot. Squares, JNK; circles, p38; triangles, ERK; diamonds, phospho-ERK. (**B**) Western blot, including ERK and phospho-ERK expression in the presence of the MEK 1/2 inhibitor UO126 (10 μM).

radiation-induced apoptosis (Table 4). Neither did they inhibit the ability of $dmPGE_2$ to attenuate apoptosis. Taken together, these data suggest that radiation-induced apoptosis in HCT-116 cells is primarily regulated through the PI3K/AKT pathway with little cross-talk to the MAPK pathways.

Discussion

We previously demonstrated that PGE_2 reduces radiation-induced apoptosis in the mouse small intestine and that endogenous PGE_2 in the intestine increases epithelial crypt survival after radiation (17). Here we report that the effects of PGE_2 in reducing radiation-induced apoptosis in the intestine are mediated by signaling through EP_2, the phosphorylation of AKT, and the inhibition of bax translocation.

In the mouse intestine, bax is expressed in the epithelial cells of the lower crypt (27–29). In these cells, irradiation induces increased bax expression, which is followed by apoptosis (28). Positional analysis of radiation-induced apoptosis demonstrates that there is less apoptosis in *Bax*$^{-/-}$ mice than in WT mice and that the difference is confined to those cells in the part of the crypt (approximate cell positions 2–8) that express bax. In the upper part of the crypt (approximate cell positions 10–20), where bax is not expressed, radiation-induced apoptosis is identical in WT and *Bax*$^{-/-}$ mice. In WT mice, $dmPGE_2$ reduces apoptosis at cell positions 3–5, but not in the mid- and upper crypt; however, in *Bax*$^{-/-}$ mice, $dmPGE_2$ has no effect on apoptosis at any position. A comparison of apoptosis in WT and *Bax*$^{-/-}$ mice indicates that bax-dependent apoptosis occurs in cell positions 6–8, yet $dmPGE_2$ did not reduce apoptosis in this compartment. The EP_2 receptor is expressed by these cells (9), which suggests that in this compartment PI3K/AKT signaling may not be as influential in determining apoptosis. Indeed, Gauthier et al. (46) found that undifferentiated Caco-2/15 cells were more sensitive to LY294002-induced apoptosis than differentiated Caco-2/15 cells. Taken together, these data indicate that in WT mice there is both bax-dependent and bax-independent apoptosis in the lower crypt but only bax-independent apoptosis in the upper crypt and that $dmPGE_2$ selectively blocks bax-dependent apoptosis in the lower crypt.

Crypt survival after radiation injury is dependent on the survival of 1 or more stem cells that are located at approximately position 4 in the lower crypt. The effects of $dmPGE_2$ and bax expression on crypt survival are consistent with the effects of $dmPGE_2$ and bax expression on apoptosis. There is both bax-dependent and bax-independent apoptosis at position 4, which results in both bax-dependent and bax-independent crypt survival. Treatment with $dmPGE_2$ decreases apoptosis at position 4 in WT but not in *Bax*$^{-/-}$ mice; as a result, treatment with $dmPGE_2$ increases crypt survival in WT mice but not in *Bax*$^{-/-}$ mice.

Bax mediates apoptosis induced by chemotherapeutic agents in intestinal epithelial cells (36). Bax is also important in mediating intestinal epithelial apoptosis in response to massive resection. In WT mice, resection of 50% of the small intestine results in an adaptive response marked by apoptosis, enhanced cell proliferation, and enhanced migration; however, in *Bax*$^{-/-}$ mice, there is no apoptotic response after 50% resection (47). Bax translocation mediates radiation-induced apoptosis in mouse thymocytes (37). Gene therapy to upregulate bax expression enhances tumor susceptibility to radiation therapy (25). Despite the clear role of bax in mediating apoptosis in intestinal cells and in mediating radiation-induced apoptosis in cell lines derived from other organs, a role for bax in radiation-induced apoptosis in the intestine had not previously been demonstrated. Pritchard et al. investigated radiation-induced apoptosis in the small intestine in WT and *Bax*$^{-/-}$ mice receiving 1 Gy and 8 Gy (38). After 1 Gy, WT and *Bax*$^{-/-}$ mice had identical levels of apoptosis, whereas after 8 Gy, there was less apoptosis in the *Bax*$^{-/-}$ mice and the difference approached statistical significance ($P = 0.063$). Crypt survival was not assessed in that study. We found significant decreases in apoptosis in *Bax*$^{-/-}$ mice compared with WT mice at both 8 Gy (data not shown) and 12 Gy. The explanation for the difference between this study and the earlier study is not clear. The genetic construct for the *Bax*$^{-/-}$ mice was identical in the 2 studies. One distinction is that we had a larger number of mice in the *Bax*$^{-/-}$ test group ($n = 6$–7, 60 half-crypts scored; vs. $n = 4$, 50 half-crypts scored, in the earlier study). It is possible that the use of a larger test group in the earlier study would have resulted in a statistically significant difference between the *Bax*$^{-/-}$ and the WT mice after 8 Gy. Our finding of reduced apoptosis in irradiated *Bax*$^{-/-}$ mice is consistent with the work of Lund's group with IGF-1 transgenic mice (48). One target organ for IGF-1 is the small-intestinal epithelium, where it increases crypt cell proliferation and decreases bax expression. In the IGF-1 transgenic mouse, there was diminished spontaneous and radiation-induced apoptosis. This decrease in radiation-induced apoptosis correlated with a decrease in bax expression in the lower crypt.

Table 4
MAPK inhibitors do not alter apoptosis in irradiated HCT-116 cells

Treatment	No inhibitor (%)	SB203580 (%)	UO126 (%)	SP600125 (%)
Vehicle	7.6 ± 0.3	6.5 ± 0.1[A]	8.8 ± 0.4	9.7 ± 0.8
$dmPGE_2$	5.6 ± 0.3	5.2 ± 0.1	7.6 ± 0.8	6.4 ± 0.5
6 Gy	20.0 ± 1.0	26.6 ± 2.4	17.8 ± 1.0	20.0 ± 1.1
6 Gy + $dmPGE_2$	9.3 ± 0.4	6.5 ± 0.2[A]	7.3 ± 0.3[A]	10.3 ± 1.0

Percent apoptosis was determined as in Table 2. Before irradiation, cultures were preincubated 1 hour with p38 MAPK inhibitor SB203580 (10 μM), MEK 1/2 inhibitor UO126 (10 μM), or JNK inhibitor SP600125 (20 μM) followed by addition of 10 μM $dmPGE_2$ as indicated. Data are the average ± SEM (n = 6–9) determined from at least 2 separate experiments. [A]$P < 0.005$ compared with comparable treatment in no-inhibitor group.

Having demonstrated that the effects of $dmPGE_2$ on radiation-induced apoptosis in the mouse intestine are mediated through bax, we next used HCT-116 cells to define the signaling pathways through which PGE_2 binding affects bax-dependent apoptosis. Experiments with receptor-specific agonists suggest that in HCT-116 cells the induction of AKT phosphorylation by PGE_2 is mediated by signaling through EP_2. Increased AKT phosphorylation through EP_2 signaling in HCT-116 cells fits with studies in $EP_2^{-/-}$ mice in which the effects of $dmPGE_2$ on radiation-induced apoptosis were mediated through EP_2 (9). AKT phosphorylation can be induced by either PI3K-dependent or PI3K-independent pathways (reviewed in ref. 49). Both EP_2 and EP_4 signaling may be coupled to AKT activation via PI3K. HEK cells transfected with either EP_2 or EP_4 displayed a 2-fold increase in AKT phosphorylation after stimulation with PGE_2 (21). AKT phosphorylation in response to PGE_2 in both EP_2- and EP_4-transfected HEK cells was completely inhibited by wortmannin, a PI3K inhibitor; this demonstrates that signaling through either EP_2 or EP_4 can result in PI3K-dependent AKT phosphorylation (21). In HCT-116 cells, $dmPGE_2$-induced AKT phosphorylation is mediated by PI3K. Furthermore, our data indicate that the ability of $dmPGE_2$ to enhance AKT phosphorylation in HCT-116 cells occurs via EGFR transactivation. PGE_2 transactivates the EGFR in several gastrointestinal cell lines through an src-dependent mechanism (42, 43). Recently, Buchanan et al. (43) demonstrated that PGE_2 stimulates AKT phosphorylation in LS174T cells via EGFR transactivation. Similar to their findings, we show that $dmPGE_2$ treatment of HCT-116 cells results in EGFR phosphorylation and that the ability of $dmPGE_2$ to enhance AKT phosphorylation is attenuated in the presence of either the src inhibitor PP2 or the EGFR kinase inhibitor PD153035. A link between PGE_2 signaling, PI3K activation, and reduced apoptosis has previously been demonstrated in lung adenocarcinoma cells. When lung adenocarcinoma cells are transfected with COX-2 or treated with PGE_2, they become resistant to apoptosis (50). COX-2 overexpression or treatment with PGE_2 in these cells also results in activation of the PI3K/AKT pathway (50). The ability of COX-2 overexpression to enhance cell survival in lung adenocarcinoma cell lines is abrogated when a PI3K dominant negative p85 subunit is also transfected into the cells (50).

Inhibition of PI3K with LY294002 blocked the ability of $dmPGE_2$ to inhibit radiation-induced apoptosis, but inhibition of PI3K alone had no effect on radiation-induced apoptosis. In contrast, transfection with AKT siRNA not only blocked the ability of $dmPGE_2$ to inhibit radiation-induced apoptosis but also dramatically increased radiation-induced apoptosis. AKT activation is known to occur through both PI3K-dependent and PI3K-independent pathways (49). Likewise, PI3K signals to downstream effectors in addition to AKT (reviewed in ref. 51). Administration of LY294002 reduces PI3K-dependent but not PI3K-independent phosphorylation, whereas transfection with AKT siRNA reduces the substrate for both PI3K-dependent and PI3K-independent phosphorylation. Thus, the most likely explanation for the differential effect of LY294002 and AKT siRNA is that activation of AKT through PI3K-dependent and PI3K-independent phosphorylation blocks radiation-induced apoptosis, while PI3K-dependent AKT activation is required for $dmPGE_2$-mediated modulation of radiation-induced apoptosis.

Signaling through PI3K/AKT reduces apoptosis by modulating the activation of pro- and antiapoptotic bcl-2 family members (22, 23, 49, 51). Complex interactions among these proteins control mitochondrial membrane permeabilization, a pivotal step in apoptosis (30–32). Antiapoptotic members such as bcl-2 and bcl-x_L localize to the mitochondrial membrane and regulate mitochondrial integrity and cytokine release. Proapoptotic members bax, bid, and bad localize to the cytoplasm and translocate to the mitochondria in response to apoptotic stimuli. AKT inhibits apoptosis by multiple mechanisms, including activation of the antiapoptotic proteins NF-κB and cAMP response element–binding protein and inactivation of the proapoptotic proteins bad, caspase-9, and forkhead (reviewed in refs. 20, 22, 23, 49, 51). AKT activation has also been linked to the inhibition of bax-induced mitochondrial membrane permeabilization. HeLa cells transfected with a constitutively active AKT construct are resistant to apoptosis triggered by IL-3 withdrawal; in the transfected cells, IL-3 deprivation failed to induce bax conformational change and translocation to the mitochondria (33). Similarly, inhibition of AKT phosphorylation with either of the PI3K inhibitors, wortmannin or LY294002, induced bax conformational change, even in the presence of IL-3 (33). Staurosporine-induced bax translocation to the mitochondria was suppressed in HeLa cells expressing a constitutively active AKT and moderately enhanced by expression of a dominant negative AKT (34). Neither dominant negative AKT nor active AKT altered the expression of bax, bcl-2, or bcl-x_L (34). Taken together, these studies implicate the PI3K/AKT pathway in controlling bax translocation to the mitochondria. How AKT activation modulates the ability of bax to undergo conformational change and translocation remains largely unknown, as bax does not contain a typical AKT phosphorylation sequence; however, neutrophil bax is phosphorylated by exogenous AKT, and this alters its ability to undergo translocation and initiate mitochondrial membrane permeabilization (35).

Radiation induces the activation of MAPKs in a tissue-specific fashion, and activated MAPKs mediate radiation-induced apoptosis in some tissues (3–5). Radiation of HCT-116 cells activated ERK but not JNK or p38. Inhibition of ERK phosphorylation with UO126 had no effect on radiation-induced apoptosis in HCT-116 cells. These results are similar to observations in RIE-1 rat intestinal epithelial cells irradiated with 7 Gy (52). Likewise, clonogenic survival in irradiated RIE-1 cells was reduced with LY294002 but not SB203580 or UO126 (52). The absence of a role for MAPKs in mediating radiation-induced apoptosis in HCT-116 cells and RIE-1 cells raises the possibility that MAPKs are not involved in mediating radiation-induced

apoptosis in the intestine. In human jejunal explants, apoptosis was induced by both LY294002 and, to a lesser extent, PD98059 (an ERK pathway inhibitor) (53). However, PD98059-induced apoptosis was localized almost exclusively to the villus (53).

Radiation injures multiple cell types, and there has been some controversy as to whether the primary mediator of radiation-induced injury in the intestine is direct radiation injury of the epithelial cells, especially the stem cells, or radiation injury of the microvascular cells leading to ischemic injury to the epithelium (54). Positional analysis reveals that the effects of $dmPGE_2$ on radiation-induced apoptosis correspond precisely to those cells that express bax, and that the ability of $dmPGE_2$ to affect crypt survival is dependent on bax expression in the epithelial stem cells. Moreover, the effects of bax expression and $dmPGE_2$ administration on radiation-induced apoptosis in the mouse intestine and in HCT-116 cells, an epithelial cell line, are similar. This similarity supports the use of irradiated HCT-116 cells as a model for radiation injury in the intestine and also suggests that radiation-induced apoptosis in the mouse intestine is the product of a direct effect of radiation on the stem cell.

The effects of $dmPGE_2$ in inhibiting radiation-induced apoptosis in the small intestine are mediated through binding to EP_2, phosphorylation of AKT, and inhibition of bax translocation from the cytoplasm to the mitochondria. These findings suggest that the in vivo administration of $dmPGE_2$ or other agents that increase AKT phosphorylation should reduce injury to the small intestine during radiation therapy. These agents might also make epithelial cancers resistant to radiation therapy. While inhibition of the synthesis of endogenous PGE_2 by nonselective NSAIDs should increase radiation-induced apoptosis in both epithelial cancers and normal intestine, selective COX-2 inhibition may be especially beneficial, because COX-2 is widely expressed in colon cancers but not in normal colon or small intestine and thus selective inhibition of COX-2 should enhance apoptosis in cancer cells but not in normal epithelium. These findings also suggest that cancers with mutations that inactivate bax and block its translocation to the mitochondria might be resistant to radiation and that NSAIDs would be ineffective in promoting apoptosis in cancers with bax mutations.

Methods

Mice. WT and bax-deficient mice on the C57BL/6 background were obtained using founders from S. Korsmeyer (Dana Farber Cancer Institute, Boston, Massachusetts, USA). Mice were maintained on a 12-hour light/dark schedule and fed standard laboratory mouse chow. Animal procedures were conducted in accordance with the Institutional Review Board at Washington University School of Medicine. Whole-body irradiation of mice was carried out in a Gammacell 40 ^{137}Cs irradiator (Atomic Energy of Canada Ltd.) at a dose rate of 80.7 cGy/min and a total dose of 12 Gy. As appropriate, animals were treated with $dmPGE_2$ (Sigma-Aldrich) dissolved in ethanol and diluted into sterile 5% sodium bicarbonate immediately before use; it was given as a single dose (0.5 mg/kg) injected i.p. at 1 hour before irradiation.

Crypt survival in mouse small intestine. Crypt survival was measured in animals killed 3.5 days after irradiation as described previously (55) using a modification of the microcolony assay (56, 57); signal detection used 3,3′-diaminobenzidine tetrahydrochloride (Sigma-Aldrich).

Apoptosis in mouse small intestine. Mice were killed 6 hours after receiving 12 Gy whole-body irradiation, and their intestines were dissected and fixed in Bouin's fixative. The proximal jejunum was divided into 5-mm segments, embedded in paraffin, and used for immunohistochemical analysis. In each set of experiments, WT and $Bax^{-/-}$ mice were treated, fixed, and scored at the same time. Apoptosis was assessed by morphological criteria using H&E-stained tissue as described by Pritchard et al. (38). Apoptosis was scored on a cell-positional basis by light microscopic analysis of 60 half-crypt sections per mouse with at least 4 mice in each group. All crypts chosen were at least 20 cells in length, with cell position 1 located at the crypt base.

Cell culture and treatment. HCT-116 cells (American Type Culture Collection), HCT-116 p21 parental cells, HCT-116 $Bax^{+/-}$ cells, and HCT-116 $Bax^{-/-}$ cells (all kindly supplied by B. Vogelstein, Johns Hopkins University, Baltimore, Maryland, USA) were maintained in McCoy's 5A medium (Mediatech Inc.) supplemented with 10% heat-inactivated FCS (Atlanta Biologicals). Subconfluent HCT-116 cells were irradiated (6 Gy) using a Gammacell 40 cesium irradiator. As appropriate, the cells received vehicle, 10 μM $dmPGE_2$ (Cayman Chemical Co.), or one of the EP receptor agonists, butaprost (10 μM), PGE_1 alcohol (1 μM), or 17-phenyltrinor-PGE_2 (10 μM; all from Cayman Chemical Co.), just prior to irradiation at 6 Gy. Where indicated, cells were preincubated with 10 μM src inhibitor PP2 (Calbiochem, EMD Biosciences Inc.), 1 μM EGFR kinase inhibitor PD153035 (Calbiochem, EMD Biosciences Inc.), 10 μM p38 MAPK inhibitor SB203580 (Promega Corp.), 10 μM MEK 1/2 inhibitor UO126 (Promega Corp.), 10 μM PI3K inhibitor LY294002 (Cell Signaling Technology Inc.), or 20 μM JNK inhibitor SP600125 (Alexis Biochemicals) for 1 hour prior to irradiation. At the indicated times after radiation, the cells were harvested for analysis of apoptosis or protein expression.

Western blotting. Western analysis was used to evaluate the phosphorylation status of AKT (Ser 473), p38 MAPK (Tyr 182), p42/p44 ERK (Thr 202/Tyr 204), JNK (Thr 183/Tyr 185), and EGFR (Tyr 1068). Antibodies for analysis of MAPKs, EGFR, and AKT expression and phosphorylation were from Santa Cruz Biotechnology Inc. or Cell Signaling Technology Inc. EP receptor expression (antibodies from Cayman Chemical Co.), bcl-x expression, and bax expression (antibodies from Santa Cruz Biotechnology Inc. or Cell Signaling Technology Inc.) in HCT-116 cells were determined by Western blotting. Typically, 10–20 μg protein was separated by SDS-PAGE, blotted to Immobilon-P membrane (Millipore Corp.), blocked, and probed with the primary antibody of interest following the supplier's suggested protocol. Following incubation with the appropriate secondary antibody, positive bands were visualized by chemiluminescence using ECL reagent (Amersham Biosciences Corp.). Densitometry was performed using NIH Image on film exposures in which image analysis indicated that pixel density was within the linear range of the film.

Apoptosis in HCT-116 cells. Exponentially growing HCT-116 or HCT-116 $Bax^{-/-}$ cells were seeded in 25 cm^2 flasks at the density of 1×10^6 to 2×10^6 cells and incubated for 18 hours. After that period, fresh medium containing 0.001% vol/vol of DMSO or 10 μM $dmPGE_2$ was added to the flasks, and cells were either irradiated or not irradiated with a dose of 6 Gy and then incubated further for 24 hours at 37°C and 5% CO_2. Floating and adherent cells were harvested by centrifugation, fixed in 70% vol/vol ice-cold ethanol in PBS, and stored at –20°C until analysis. Apoptosis was determined by flow cytometry using an annexin V–FITC and propidium iodide staining kit (Roche Diagnostics Corp.), according to the manufacturer's instructions. As a control, apoptosis was also measured in HCT-116 p21 parental and HCT-116 $Bax^{+/-}$ cell lines at 0 Gy, 6 Gy, or 6 Gy plus 10 μM $dmPGE_2$. Similar experiments measuring apoptosis were also performed with HCT-116 cultures preincubated for 1 hour with 10 μM SB203580, 10 μM UO126, 20 μM SP600125, or 10 μM LY294002 followed by addition of DMSO (final concentration less than 0.005%) or 10 μM $dmPGE_2$ before irradiation.

Bax translocation. HCT-116 cells (2×10^7) were seeded in 75 cm^2 flasks and cultured overnight. Thereafter, cell cultures were treated with 0.005% vol/vol of DMSO or 10 μM of $dmPGE_2$, irradiated or not irradiated at 6 Gy, and incubated for 24 hours as described above for apoptosis studies. Adherent cells were harvested and processed for fractionation into cytosolic and mitochondrial fractions using a kit from BioVision Inc. Forty micrograms

of protein from cytosolic fractions and 100 μg protein from mitochondrial fractions were separated by gel electrophoresis (10% Novex SDS-PAGE; Invitrogen Corp.) and transferred to a PVDF membrane. Antibodies used were rabbit anti-bax (N-20) and mouse anti–α-tubulin (both from Santa Cruz Biotechnology Inc.), diluted 1:100; and rabbit anti–voltage-dependent anion-selective channel protein-1 (Calbiochem, EMD Biosciences Inc.), diluted 1:1,000. Both donkey anti-rabbit (1:2,000) and sheep anti-mouse (1:3,000) peroxidase-labeled secondary antibodies were purchased from Amersham Biosciences Corp.

Transfections and use of siRNA. All transfections were done using Lipofectamine 2000 (Invitrogen Corp.) diluted in Opti-MEM I (Invitrogen Corp.) according to the manufacturer's instructions. For plasmid DNA transfections, cells were incubated with 2 μg of plasmid DNA for 24 hours. Cells were then allowed to recover for a further 24 hours before selection of resistant clones in McCoy's medium containing 1 mg/ml G418. The plasmid used for transfections was either the constitutively active myrAKT (a kind gift of P. Stahl, Washington University School of Medicine, St. Louis, Missouri, USA) or the control empty plasmid pcDNA 3.1 (Invitrogen Corp.). Exponentially growing pcDNA or myrAKT transfectants (1×10^6 to 2×10^6) were seeded in 25 cm^2 flasks and incubated for 18 hours. Fresh medium was added after that period, and cells were irradiated or not irradiated with a dose of 6 Gy, harvested 24 hours later, and processed for apoptosis determination by FACS analysis after annexin V–FITC and propidium iodide staining as described above.

For siRNA experiments, 40–50% confluent cells in 25 cm^2 flasks were incubated for 24 hours in the presence of 100 nM Smartpool Plus AKT siRNA or 100 nM scrambled SMARTpool siRNA control (Dharmacon Inc.). Transfectants were incubated for a further 24 hours in the presence of fresh medium. Then new medium containing DMSO or 10 μM of $dmPGE_2$ was added, and the cells were used for radiation-induced apoptosis experiments as described above.

Statistical analyses. One-way ANOVA was used to determine statistical significance for differences in positional apoptotic index. Student's 2-tailed *t* test was used for statistical analysis of other data.

Acknowledgments

This work was supported by NIH grants DK33165 (to W.F. Stenson) and DK62265 (to S. Anant) and by the Washington University Digestive Disease Research Core Center.

Received for publication May 20, 2004, and accepted in revised form September 21, 2004.

Address correspondence to: Teresa G. Tessner, Division of Gastroenterology, Washington University School of Medicine, Campus Box 8124, 660 South Euclid Street, St. Louis, Missouri 63110, USA. Phone: (314) 362-8953; Fax: (314) 362-9035; E-mail: stensnlb@im.wustl.edu.

1. Potten, C.S. 1998. Stem cells in gastrointestinal epithelium: numbers, characteristics, and death. *Philos. Trans. R. Soc. Lond. B Biol. Sci.* **353**:821–830.
2. Pritchard, D.M., and Watson, A.J.M. 1996. Apoptosis and gastrointestinal pharmacology. *Pharmacol. Ther.* **72**:149–169.
3. Schmidt-Ullrich, R.K., Dent, P., Grant, S., Mikkelsen, R.B., and Valerie, K. 2000. Signal transduction and cellular radiation responses. *Radiat. Res.* **153**:245–257.
4. Dent, P., et al. 2003. Stress and radiation-induced activation of multiple intracellular signaling pathways. *Radiat. Res.* **159**:283–300.
5. Dent, P., Yacoub, A., Fisher, P.B., Hagan, M.P., and Grant, S. 2003. MAPK pathways in radiation responses. *Oncogene.* **22**:5885–5896.
6. Hanson, W.R., and Thomas, C. 1983. 16,16-Dimethyl prostaglandin E_2 increases survival of murine intestinal stem cells when given before photon radiation. *Radiat. Res.* **96**:393–398.
7. Hanson, W.R., and Ainsworth, E.J. 1985. 16,16-Dimethyl prostaglandin E_2 induces radioprotection in murine intestinal and hematopoietic stem cells. *Radiat. Res.* **103**:196–203.
8. Houchen, C.W., Stenson, W.F., and Cohn, S.M. 2000. Disruption of cyclooxygenase-1 gene results in an impaired response to radiation injury. *Am. J. Physiol. Gastrointest. Liver Physiol.* **279**:G858–G865.
9. Houchen, C.W., Sturmoski, M.A., Anant, S., Breyer, R.M., and Stenson, W.F. 2003. Prosurvival and antiapoptotic effects of PGE_2 in radiation injury are mediated by EP_2 receptor in intestine. *Am. J. Physiol. Gastrointest. Liver Physiol.* **284**:G490–G498.
10. Lee, T.K., and Stupan, I. 2002. Radioprotection: the non-steroidal anti-inflammatory drugs (NSAIDs) and prostaglandins. *J. Pharm. Pharmacol.* **54**:1435–1445.
11. Choy, H., and Milas, L. 2003. Enhancing radiotherapy with cyclooxygenase-2 enzyme inhibitors: a rational advance? *J. Natl. Cancer Inst.* **95**:1440–1452.
12. Milas, L., et al. 1999. Enhancement of tumor response to γ-radiation by an inhibitor of cyclooxygenase-2 enzyme. *J. Natl. Cancer Inst.* **91**:1501–1504.
13. Kishi, K., et al. 2000. Preferential enhancement of tumor radioresponse by a cyclooxygenase-2 inhibitor. *Cancer Res.* **60**:1326–1331.
14. Petersen, C., Petersen, S., Milas, L., Lange, F.F., and Tofilon, P.J. 2000. Enhancement of intrinsic tumor cell radiosensitivity induced by a selective cyclooxygenase-2 inhibitor. *Clin. Cancer Res.* **6**:2513–2520.
15. Pyo, H., et al. 2001. A selective cyclooxygenase-2 inhibitor, NS-398, enhances the effect of radiation in vitro and in vivo preferentially on the cells that express cyclooxygenase-2. *Clin. Cancer Res.* **7**:2998–3005.
16. Davis, T.W., et al. 2004. Synergy between celecoxib and radiotherapy results from inhibition of cyclooxygenase-2-derived prostaglandin E_2, a survival factor for tumor and associated vasculature. *Cancer Res.* **64**:279–285.
17. Cohn, S.M., Schloemann, S., Tessner, T., Seibert, K., and Stenson, W.F. 1997. Crypt stem cell survival in the mouse intestinal epithelium is regulated by prostaglandins synthesized through cyclooxygenase-1. *J. Clin. Invest.* **99**:1367–1379.
18. Narumiya, S., Sugimoto, Y., and Ushikubi, F. 1999. Prostanoid receptors: structures, properties, and functions. *Physiol. Rev.* **79**:1193–1226.
19. Regan, J.W. 2003. EP_2 and EP_4 prostanoid receptor signaling. *Life Sci.* **74**:143–153.
20. Datta, S.R., Brunet, A., and Greenberg, M.E. 1999. Cellular survival: a play in three Akts. *Genes Dev.* **13**:2905–2927.
21. Fujino, H., West, K.A., and Regan, J.W. 2002. Phosphorylation of glycogen synthase kinase-3 and stimulation of T-cell factor signaling following activation of EP_2 and EP_4 prostanoid receptors by prostaglandin E_2. *J. Biol. Chem.* **277**:2614–2619.
22. Kim, R., et al. 2002. Current status of the molecular mechanisms of anticancer drug-induced apoptosis. *Cancer Chemother. Pharmacol.* **50**:343–352.
23. Chang, F., et al. 2003. Involvement of PI3K/AKT pathway in cell cycle progression, apoptosis, and neoplastic transformation: a target for cancer chemotherapy. *Leukemia.* **17**:590–603.
24. Chong, M.J., et al. 2000. Atm and bax cooperate in ionizing radiation-induced apoptosis in the central nervous system. *Proc. Natl. Acad. Sci. U. S. A.* **97**:889–894.
25. Arafat, W.O., et al. 2000. An adenovirus encoding proapoptotic bax induces apoptosis and enhances the radiation effect in human ovarian cancer. *Mol. Ther.* **1**:545–554.
26. Ahmed, M.M., et al. 2002. Restoration of transforming growth factor-β signaling enhances radiosensitivity by altering the bcl-2/bax ratio in the p53 mutant pancreatic cancer cell line MIA PaCa-2. *J. Biol. Chem.* **277**:2234–2246.
27. Krajewski, S., et al. 1994. Immunohistochemical determination of in vivo distribution of bax, a dominant inhibitor of bcl-2. *Am. J. Pathol.* **145**:1323–1336.
28. Kitada, S., Krajewski, S., Miyashita, T., Krajewska, M., and Reed, J.C. 1996. γ-Radiation induces upregulation of bax protein and apoptosis in radiosensitive cells in vivo. *Oncogene.* **12**:187–192.
29. Aschoff, A.P., Ott, U., Funfstuck, R., Stein, G., and Jirikowski, G.F. 1999. Colocalization of BAX and BCL-2 in small intestine and kidney biopsies with different degrees of DNA fragmentation. *Cell Tissue Res.* **296**:351–357.
30. Gross, A., McDonnell, J.M., and Korsmeyer, S.J. 1999. BCL-2 family members and the mitochondria in apoptosis. *Genes Dev.* **13**:1899–1911.
31. Scorrano, L., and Korsmeyer, S.J. 2003. Mechanisms of cytochrome c release by proapoptotic BCL-2 family members. *Biochem. Biophys. Res. Commun.* **304**:437–444.
32. Esposti, M.D., and Dive, C. 2003. Mitochondrial membrane permeabilization by Bax/Bak. *Biochem. Biophys. Res. Commun.* **304**:455–461.
33. Yamaguchi, H., and Wang, H.G. 2001. The protein kinase PKB/Akt regulates cell survival and apoptosis by inhibiting bax conformational change. *Oncogene.* **20**:7779–7786.
34. Tsuruta, F., Masuyama, N., and Gotoh, Y. 2002. The phosphatidylinositol 3-kinase (PI3K)-Akt pathway suppresses bax translocation to mitochondria. *J. Biol. Chem.* **277**:14040–14047.
35. Gardai, S.J., et al. 2004. Phosphorylation of bax serine184 by Akt regulates its activity and apoptosis in neutrophils. *J. Biol. Chem.* **279**:21085–21095.
36. Zhang, L., Yu, J., Park, B.H., Kinzler, K.W., and Vogelstein, B. 2000. Role of BAX in the apoptotic response to anticancer agents. *Science.* **290**:989–992.
37. Hsu, Y.-T., Wolter, K.G., and Youle, R.J. 1997. Cytosol-to-membrane redistribution of Bax and Bcl-X_L

during apoptosis. *Proc. Natl. Acad. Sci. U. S. A.* **94**:3668–3672.
38. Pritchard, D.M., Potten, C.S., Korsmeyer, S.J., Roberts, S., and Hickman, J.A. 1999. Damage-induced apoptosis in intestinal epithelia from bcl-2-null and bax-null mice: investigations of the mechanistic determinants of epithelial apoptosis in vivo. *Oncogene.* **18**:7287–7293.
39. Belley, A., and Chadee, K. 1999. Prostaglandin E_2 stimulates rat and human colonic mucin exocytosis via the EP_4 receptor. *Gastroenterology.* **117**:1352–1362.
40. Sheng, H., Shao, J., Washington, M.K., and Dubois, R.N. 2001. Prostaglandin E_2 increases growth and motility of colorectal carcinoma cells. *J. Biol. Chem.* **276**:18075–18081.
41. Fukuda, R., Kelly, B., and Semenza, G.L. 2003. Vascular endothelial growth factor gene expression in colon cancer cells exposed to prostaglandin E_2 is mediated by hypoxia-inducible factor 1. *Cancer Res.* **63**:2330–2334.
42. Pai, R., et al. 2002. Prostaglandin E_2 transactivates EGF receptor: a novel mechanism for promoting colon cancer growth and gastrointestinal hypertrophy. *Nat. Med.* **8**:289–293.
43. Buchanan, F.G., Wang, D., Bargiacchi, F., and Dubois, R.N. 2003. Prostaglandin E_2 regulates cell migration via the intracellular activation of the epidermal growth factor receptor. *J. Biol. Chem.* **278**:35451–35457.
44. Katso, R., et al. 2001. Cellular function of phosphoinositide 3-kinases: implications for development, immunity, homeostasis, and cancer. *Annu. Rev. Cell Dev. Biol.* **17**:615–675.
45. Welch, H.C.E., Coadwell, W.J., Stephens, L.R., and Hawkins, P.T. 2003. Phosphoinositide 3-kinase-dependent activation of Rac. *FEBS Lett.* **546**:93–97.
46. Gauthier, R., et al. 2001. Human intestinal epithelial cell survival: differentiation state-specific control mechanisms. *Am. J. Physiol. Cell Physiol.* **280**:C1540–C1554.
47. Tang, Y., et al. 2004. Bax is required for resection-induced changes in apoptosis, proliferation, and members of the extrinsic cell death pathways. *Gastroenterology.* **126**:220–230.
48. Wilkins, H.R., et al. 2002. Reduction of spontaneous and irradiation-induced apoptosis in small intestine of IGF-1 transgenic mice. *Am. J. Physiol. Gastrointest. Liver Physiol.* **283**:G457–G464.
49. Kandel, E.S., and Hay, N. 1999. The regulation and activities of the multifunctional serine/threonine kinase Akt/PKB. *Exp. Cell Res.* **253**:210–229.
50. Lin, M.T., Lee, R.C., Yang, P.C., Ho, F.M., and Kuo, M.L. 2001. Cyclooxygenase-2 inducing Mcl-1-dependent survival mechanism in human lung adenocarcinoma CL1.0 cells. *J. Biol. Chem.* **276**:48997–49002.
51. Vivanco, I., and Sawyers, C.L. 2002. The phosphatidylinositol 3-kinase-AKT pathway in human cancer. *Nat. Rev.* **2**:489–501.
52. Grana, T.M., Rusyn, E.V., Zhou, H., Sartor, C.I., and Cox, A.D. 2002. Ras mediates radioresistance through both phosphatidylinositol 3-kinase-dependent and raf-dependent but mitogen-activated protein kinase/extracellular signal-regulated kinase kinase-independent signaling pathways. *Cancer Res.* **62**:4142–4150.
53. Gauthier, R., et al. 2001. Differential sensitivity to apoptosis between the human small and large intestinal mucosae: linkage with segment-specific regulation of BCL-2 homologs and involvement of signaling pathways. *J. Cell. Biochem.* **82**:339–355.
54. Paris, F., et al. 2001. Endothelial apoptosis as the primary lesion initiating intestinal radiation damage in mice. *Science.* **293**:293–297.
55. Riehl, T., Cohn, S., Tessner, T., Schloemann, S., and Stenson, W.F. 2000. Lipopolysaccharide is radioprotective in the mouse intestine through a prostaglandin-mediated mechanism. *Gastroenterology.* **118**:1106–1116.
56. Potten, C.S., Merritt, A., Hickman, J., Hall, P., and Faranda, A. 1994. Characterization of radiation-induced apoptosis in the small intestine and its biological implications. *Int. J. Radiat. Biol.* **65**:71–78.
57. Withers, H.R., and Elkind, M.M. 1970. Microcolony survival assay for cells of mouse intestinal mucosa exposed to radiation. *Int. J. Radiat. Biol.* **17**:261–267.